Research Square

Preprints are preliminary reports that have not undergone peer review.
They should not be considered conclusive, used to inform clinical practice,
or referenced by the media as validated information.

Seam Geometry of Bohmian Mechanics: Geodesics, Foliations, and Nodal Singularities

Lars Rönnbäck

lars@uptochange.com

Stockholm University

Research Article

Keywords: Bohmian mechanics, Madelung hydrodynamics, seam geometry, quantum potential, quadratic differentials, nodal singularities

Posted Date: March 4th, 2026

DOI: https://doi.org/10.21203/rs.3.rs-8968273/v1

License: This work is licensed under a Creative Commons Attribution 4.0 International License.
Read Full License

Additional Declarations: No competing interests reported.

Seam Geometry of Bohmian Mechanics: Geodesics, Foliations, and Nodal Singularities

Lars Rönnbäck (ORCID: 0000-0002-8810-7587)[1*]

[1*]Department of Computer and Systems Sciences, Stockholm University, Stockholm, Sweden.

Corresponding author(s). E-mail(s): lars@uptochange.com;

Abstract

This paper reframes Bohmian mechanics in seam variables built from the wavefunction modulus and phase. Writing $\psi = R\exp(iS/\hbar)$, the amplitude seam $s = \log R$ encodes the Bohm–Madelung quantum potential via $Q = -(R''/R) = -(s'' + (s')^2)$ in the stationary one-dimensional (1D) convention used here. An effective seam $\tilde{s} := S - \frac{1}{2}s$ defines a seam-induced conformal factor that serves as a prototype for higher-dimensional metric constructions.

Assuming a complex coordinate $z = x + iy$ on a two-dimensional (2D) configuration plane, the quadratic differential (QD) $w = (\partial_z^2 \log\psi)\,dz^2$ is introduced and its induced horizontal direction field is compared to probability-current streamlines. For the Gaussian vortex state $\psi = ze^{-|z|^2/2}$, exact alignment is proved: away from the node, the QD-horizontal direction field coincides with the probability-current direction field. More generally, a local "vortex dominance" proposition gives asymptotic direction-field alignment near any isolated simple node under a mild factorisation hypothesis, and explicit limitations are documented via a two-node non-example.

Reproducible numerical tests for a centered vortex, a shifted vortex, and a two-node state quantify when alignment persists and when it fails.

Keywords: Bohmian mechanics, Madelung hydrodynamics, seam geometry, quantum potential, quadratic differentials, nodal singularities

1 Introduction

The seam framework generates geometric quantities from a scalar field s via explicit local rules. Here we apply this scalar-first viewpoint to the Madelung–Bohm formulation.

Let $\psi = R\exp(iS)$, in natural units $\hbar = 1$ (and with $m = 1$ when interpreting S as a phase/action). The amplitude seam is $s = \log R$, so that $R''/R = s'' + (s')^2$ in 1D (and $\Delta R/R = \Delta s + |\nabla s|^2$ in higher dimensions). Bohmian trajectories obey $\dot{x} = \nabla S$.

We introduce the effective seam

$$\tilde{s} := S - \tfrac{1}{2}s,$$

which induces a conformal metric of the form $g = |\nabla\tilde{s}|^2\delta_{ij}$. A second (partly conjectural) geometric layer comes from the complex logarithm $f := \log\psi = s + iS$ and the quadratic differential $w := (\partial_z^2 \log\psi)\,dz^2$ after analytic continuation of ψ.

All formal statements below are made for the stationary 1D case (most explicit calculations). Higher-dimensional generalisations using level-set foliations of s are noted separately.

Structure of the paper. We first establish seam identities that reframe the Bohm–Madelung system in terms of $s = \log R$ and $\tilde{s} = S - \frac{1}{2}s$, including the stationary quantum potential identity $Q = -(s'' + (s')^2)$. We then introduce the quadratic differential $w = \partial_z^2 \log\psi\, dz^2$, prove exact and asymptotic alignment results for vortex-type nodes, and record explicit limitations and non-examples. Finally, we discuss nodal singularities and supporting numerical tests.

2 Setup and Conventions

Definition 2.1 (Seam geometry in this paper) By *seam geometry* we mean the construction of geometric quantities from a scalar field (a *seam*) via explicit local rules. In the present setting the wavefunction ψ provides seams through its polar form $\psi = Re^{iS}$: the amplitude seam $s := \log R$ and the effective seam $\tilde{s} := S - \frac{1}{2}s$. The main seam-generated objects used below are the quantum potential identity $Q = -(s'' + (s')^2)$ in 1D (and $Q = -(\Delta s + |\nabla s|^2)$ formally in higher dimensions), the seam-induced conformal factor $|\nabla\tilde{s}|^2$, and the quadratic differential $w = (\partial_z^2 \log\psi)\,dz^2$.

We work primarily with the stationary Schrödinger equation in 1D in the convention

$$-\psi''(x) + V(x)\,\psi(x) = E\,\psi(x), \tag{2.1}$$

and write

$$\psi(x) = R(x)e^{iS(x)}, \qquad R(x) > 0 \text{ away from nodes.} \tag{2.2}$$

Define the amplitude seam $s := \log R$. A direct substitution of eq. (2.2) into eq. (2.1) yields the Bohm–Madelung system [1–3]

$$(S')^2 + V + Q = E, \tag{2.3}$$

$$(R^2 S')' = 0, \tag{2.4}$$

where the (stationary) quantum potential is

$$Q := -\frac{R''}{R} = -(s'' + (s')^2). \tag{2.5}$$

The Bohmian velocity field is $\dot{x} = S'(x)$.

Remark 2.2 (Schrödinger ODE as a projective connection (1D)) Rewrite eq. (2.1) as a second-order linear ODE

$$\psi''(x) + (E - V(x))\,\psi(x) = 0.$$

It is a classical fact from Sturm–Liouville theory and projective differential geometry [11] that if ψ_1, ψ_2 are two linearly independent solutions and $F := \psi_1/\psi_2$, then the Schwarzian derivative

$$\mathcal{S}(F, x) := \frac{F'''}{F'} - \frac{3}{2}\left(\frac{F''}{F'}\right)^2$$

satisfies

$$\mathcal{S}(F, x) = 2\,(E - V(x)).$$

Equivalently, the coefficient $E - V$ defines a projective connection on the x-line. This remark is included only as context for the appearance of Schwarzian/projective structures in nearby mathematics; the main object used in the present paper remains $w = \partial_z^2 \log \psi$.

Remark 2.3 (Higher-dimensional seam identity (formal extension)) In d dimensions one has the elementary identity

$$\frac{\Delta R}{R} = \Delta(\log R) + |\nabla(\log R)|^2 = \Delta s + |\nabla s|^2, \tag{2.6}$$

valid wherever $R > 0$. For the stationary Schrödinger convention $-\Delta\psi + V\psi = E\psi$ (natural units), the Bohm quantum potential takes the form

$$Q = -\frac{\Delta R}{R} = -(\Delta s + |\nabla s|^2),$$

so the Hamilton–Jacobi equation can be written suggestively as

$$|\nabla S|^2 + V - \Delta s - |\nabla s|^2 = E.$$

This paper keeps the main derivations in 1D but uses eq. (2.6) as motivation for the geometric role of s in higher-dimensional generalisations.

Remark 2.4 (Units) Throughout we use natural units $\hbar = 1$ and (when interpreting S as an action/phase field) particle mass $m = 1$. With this convention S is dimensionless (a phase), and $s = \log R$ is dimensionless, so the effective seam $\tilde{s} := S - \frac{1}{2}s$ is dimensionless as written.

3 Effective Seam and a 1D Geodesic Reformulation

Remark 3.1 (1D geodesic reformulation (reparametrisation triviality)) In stationary 1D, one may associate to the effective seam $\tilde{s} := S - \frac{1}{2}s$ the conformal metric

$$ds_g^2 := (\tilde{s}'(x))^2\,dx^2. \tag{3.1}$$

Any C^2 curve becomes an affine geodesic after reparametrisation, since in 1D every metric $ds^2 = f(x)^2 dx^2$ is isometric to the Euclidean line via $y = \int^x f(u)\,du$. Accordingly, the role of eq. (3.1) in this paper is not to claim nontrivial 1D geometry, but to exhibit an explicit seam-induced conformal factor tied to (S, s) that has meaningful higher-dimensional analogues.

Remark 3.2 (Higher-dimensional metric candidates) In more than one dimension, the effective seam suggests multiple natural metric constructions. Besides the isotropic conformal choice $g = |\nabla \tilde{s}|^2 \delta_{ij}$ used as a simple prototype in this paper, one can also consider the rank-one tensor

$$g_{ij} := \partial_i \tilde{s}\, \partial_j \tilde{s},$$

which is directly tied to the flow potential $\tilde{s}$ and may be better suited for comparing direction fields. These higher-dimensional metric choices are not pursued here.

4 Quadratic Differentials and Flow Organisation (2D/Complex Setting)

To compare with probability-current streamlines in 2D examples, we use the (standard holomorphic) Wirtinger derivative

$$\partial_z := \tfrac{1}{2}(\partial_x - i\partial_y), \qquad z = x + iy, \tag{4.1}$$

which satisfies $\partial_z z = 1$ and $\partial_z \bar{z} = 0$, and define

$$w(z)\, dz^2 := \partial_z^2 \log \psi(z)\, dz^2 \tag{4.2}$$

on regions where $\psi \neq 0$. When ψ is holomorphic in z, this recovers the usual holomorphic quadratic differential. For general real wavefunctions $\psi(x, y)$, we apply ∂_z termwise using the product rule, exploiting $\partial_z \bar{z} = 0$ to isolate the holomorphic content; eq. (4.2) should be read in this extended sense and local quadratic-differential foliation theory applies in the meromorphic-in-z regimes.

Remark 4.1 (On analytic continuation) The quadratic-differential picture is most straightforward when ψ extends to a function that is analytic (or at least meromorphic) in a complex coordinate z on the region of interest, since then $w = \partial_z^2 \log \psi$ is meromorphic away from zeros and standard local quadratic-differential foliation theory applies. In the numerical 2D examples below we regard $\psi(x, y)$ as a smooth function on the plane and apply ∂_z as a differential operator via eq. (4.1). For stationary 1D eigenfunctions, analytic continuation is standard for many common solvable models (e.g. harmonic-oscillator states extend to entire functions), but for general potentials it should be viewed as a mathematical device for organising local nodal geometry rather than a universal physical assumption.

Remark 4.2 (Projective structure, Schwarzian, and the quantum potential) Algebraically,

$$\partial_z^2 \log \psi = \frac{\partial_z^2 \psi}{\psi} - \left(\frac{\partial_z \psi}{\psi}\right)^2,$$

so w measures a kind of "curvature" of the logarithmic derivative $\partial_z\psi/\psi$. In projective differential geometry, quadratic differentials arise as components of projective connections and via the Schwarzian derivative [11]. Writing $f = \log\psi$, we have $w = \partial_z^2 f$, and the Schwarzian $\mathcal{S}(f,z) = (\partial_z^3 f)/(\partial_z f) - \frac{3}{2}\big((\partial_z^2 f)/(\partial_z f)\big)^2$ is built algebraically from $w = \partial_z^2 f$ and $\partial_z f$; this connects $w\,dz^2$ to the same projective structure already noted in Remark 2.2 for the Schrödinger equation.

There is a direct computational link to the quantum potential. Setting $f = s + iS$ and using $\psi = e^f$ gives

$$\frac{\psi''}{\psi} = f'' + (f')^2 = \big(s'' + s'^2 - S'^2\big) + i\big(S'' + 2s'S'\big),$$

so $\mathrm{Re}(\psi''/\psi) = s'' + s'^2 - S'^2 = -Q - S'^2$, where we used $Q = -(s'' + s'^2)$. The Schrödinger equation reads $\psi''/\psi = -(E - V)$ (real V, E), giving the decomposition

$$E - V = Q + S'^2.$$

This is simply the Hamilton–Jacobi equation eq. (2.3) (which reads $(S')^2 + V + Q = E$, i.e. $E - V = Q + S'^2$, confirming sign consistency), but its derivation via $f = \log\psi$ reveals the geometric content: the quantum potential is the *amplitude-curvature component* of the projective data encoded in ψ''/ψ, while the phase gradient S' carries the kinetic contribution. In this sense $w\,dz^2$ sits at the interface of seam geometry and projective differential geometry: it is the second-order component of the projective connection whose real part splits cleanly into quantum and classical energy contributions. A structurally analogous quadratic differential appears in two-dimensional conformal field theory as the holomorphic stress tensor [12], where operator insertions produce double poles; the zeros of ψ play exactly this role, as made precise in Observation 4.3 — this structural parallel motivates the geometric language but does not imply a dynamical identification with the CFT stress tensor.

Observation 4.3 (Pole structure and foliation organiser) *Assume ψ extends analytically to a complex neighbourhood of interest and that w in eq. (4.2) is meromorphic in z away from zeros of ψ. Then zeros of ψ produce double poles of w whose induced horizontal foliation provides an organiser of nodal neighbourhood geometry.*

Proof If $\psi(z) \sim (z-\rho)^m$ has a zero of order m at $z = \rho$, then

$$\log\psi(z) = m\log(z-\rho) + \text{holomorphic}, \qquad \partial_z^2 \log\psi(z) \sim -\frac{m}{(z-\rho)^2}.$$

Thus w has a double pole with residue data determined by m. By standard quadratic differential theory [7], a double pole generates a prong-type foliation whose number of distinguished directions grows linearly with m. This provides a geometric organiser for how integral curves can approach/avoid nodal points. The double-pole structure near isolated zeros is closely analogous to the phase singularities (wave vortices) studied in optics and wave-field physics [8, 9], where circulating phase and current around a node are the defining features.

In this setting the use of quadratic-differential local theory is justified once ψ is fixed as an analytic function on a complex domain: $w = \partial_z^2 \log\psi$ is then a meromorphic function away from zeros of ψ, and the induced foliation is a standard object of the theory (the branch ambiguity of $\log\psi$ only contributes an additive constant and does not affect $\partial_z^2 \log\psi$).

A full identification of "horizontal leaves" with Bohmian trajectories requires specifying (i) the map from the z-plane foliation to trajectories in configuration space, and (ii) a parameter choice along trajectories. No such global identification is attempted here; the key input is the pole/prong correspondence and the resulting local direction field near nodes. □

Observation 4.4 (Direction-field comparison with probability current) *On a 2D configuration plane with $\psi(x, y)$, define the probability current*

$$\mathbf{J} := \mathrm{Im}(\bar{\psi}\,\nabla\psi), \tag{4.3}$$

and the QD-horizontal direction angle

$$\theta_{\mathrm{qd}}(x, y) := -\tfrac{1}{2}\arg\big(w(x + iy)\big) \pmod{\pi}. \tag{4.4}$$

Where both are defined and $\mathbf{J} \neq 0$, one can meaningfully test whether current streamlines align with the QD-horizontal direction field, i.e. $\mathbf{J}/|\mathbf{J}| = \pm(\cos\theta_{\mathrm{qd}}, \sin\theta_{\mathrm{qd}})$.

Proposition 4.5 (Exact alignment for the vortex test state) *Consider the 2D vortex-like state*

$$\psi(x, y) = (x + iy)\exp\big(-(x^2 + y^2)/2\big) = z\, e^{-|z|^2/2}. \tag{4.5}$$

On $\mathbb{R}^2 \setminus \{0\}$, the probability-current direction field and the QD-horizontal direction field from eq. (4.2) coincide (up to the $\pm$ ambiguity of an unoriented foliation).

Proof Write $z = re^{i\theta}$ so that $\psi = Re^{iS}$ with phase $S = \theta$ and amplitude $R = r\, e^{-r^2/2}$. Hence

$$\nabla S = \frac{1}{r}\,\mathbf{e}_\theta, \qquad \mathbf{J} = R^2\nabla S = re^{-r^2}\,\mathbf{e}_\theta,$$

so the current streamlines are circles and the current direction is tangential ($\mathbf{e}_\theta$) on $\mathbb{R}^2 \setminus \{0\}$.

Next compute $w = \partial_z^2 \log\psi$ using eq. (4.1). Although $\psi = ze^{-|z|^2/2}$ is not holomorphic ($|z|^2 = z\bar{z}$ depends on $\bar{z}$), the identity $\partial_z\bar{z} = 0$ means non-holomorphic terms are killed by ∂_z. Concretely, since

$$\log\psi = \log z - \tfrac{1}{2}z\bar{z},$$

we have $\partial_z \log\psi = 1/z - \bar{z}/2$ (using $\partial_z(z\bar{z}) = \bar{z}$), and then

$$w = \partial_z^2 \log\psi = -\frac{1}{z^2}$$

since $\partial_z(-\bar{z}/2) = 0$. The non-holomorphic Gaussian factor therefore contributes only to the first-order term and drops out of w entirely. Thus $\arg w = \arg(-1) - 2\theta = \pi - 2\theta \pmod{2\pi}$, so

$$\theta_{\mathrm{qd}} = -\tfrac{1}{2}\arg w \equiv -\tfrac{1}{2}(\pi - 2\theta) = \theta - \tfrac{\pi}{2} \pmod{\pi}.$$

The unit vector $(\cos\theta_{\mathrm{qd}}, \sin\theta_{\mathrm{qd}})$ is exactly $\mathbf{e}_\theta$ (up to sign), which matches the current direction. This proves the claimed alignment. □

Proposition 4.6 (Local vortex dominance near an isolated simple node) *Let $\psi(x, y)$ be a C^2 complex-valued wavefunction on a neighbourhood of $z_0 \in \mathbb{C}$, and assume that ψ has an isolated simple zero at z_0 and can be written locally as*

$$\psi(z, \bar{z}) = (z - z_0)\, g(z, \bar{z}), \qquad g \neq 0 \text{ near } z_0.$$

Define $w = \partial_z^2 \log\psi$ on the punctured neighbourhood $0 < |z - z_0| < r_*$ and define θ_{qd} by eq. (4.4). Then as $r := |z - z_0| \to 0$:

- *(QD dominance) one has*

$$w(z) = -\frac{1}{(z - z_0)^2} + \partial_z^2 \log g(z, \bar{z}),$$

and in particular if $\sup_{|z-z_0|\le r_*} |\partial_z^2 \log g| \le M$ then for sufficiently small r,

$$\theta_{\mathrm{qd}}(z) \equiv \arg(z - z_0) - \tfrac{\pi}{2} \pmod{\pi}$$

up to an angular error $O(Mr^2)$.

- *(Current direction) writing $\psi = Re^{iS}$ on the punctured neighbourhood, the probability current satisfies $\mathbf{J} = R^2 \nabla S$. Moreover*

$$S(z) = \arg(z - z_0) + \mathrm{Im}(\log g(z, \bar{z}))$$

so $\nabla S = r^{-1}\mathbf{e}_\theta + O(1)$ as $r \to 0$, and the unit current direction $\mathbf{J}/|\mathbf{J}|$ (where defined) approaches the tangential direction $\mathbf{e}_\theta$ with angular error $O(r)$.

Consequently, in any sufficiently small punctured neighbourhood of z_0 where $\mathbf{J} \neq 0$, the QD-horizontal direction field and the current direction field align asymptotically as $r \to 0$.

Proof Using $\log \psi = \log(z - z_0) + \log g$ on the punctured neighbourhood, differentiation gives

$$\partial_z^2 \log \psi = -\frac{1}{(z - z_0)^2} + \partial_z^2 \log g,$$

which proves the first displayed identity. Writing

$$w(z) = -\frac{1}{(z - z_0)^2}\Big(1 - (z - z_0)^2\, \partial_z^2 \log g(z, \bar{z})\Big)$$

shows that if $|(z - z_0)^2\, \partial_z^2 \log g| \leq Mr^2$ is small then the argument of w differs from that of $-(z - z_0)^{-2}$ by $O(Mr^2)$, and therefore the QD-horizontal angle differs from $\arg(z - z_0) - \pi/2$ by the same order (mod π).

For the current, write $\psi = Re^{iS}$ with $S = \mathrm{Im}(\log \psi) = \arg(z - z_0) + \mathrm{Im}(\log g)$. The gradient of $\arg(z - z_0)$ is $r^{-1}\mathbf{e}_\theta$ while $\nabla \mathrm{Im}(\log g)$ is bounded because $g \neq 0$ and g is C^2. Thus $\nabla S = r^{-1}\mathbf{e}_\theta + O(1)$, and normalising yields an angular deviation from $\mathbf{e}_\theta$ of order $O(r)$. Since $\mathbf{J} = R^2 \nabla S$, the current direction agrees with the direction of ∇S wherever $\mathbf{J} \neq 0$. □

Conjecture 4.7 (Single-vortex dominance on annuli (refined target)) *Let $\psi(x, y)$ be a smooth, complex-valued wavefunction on a planar region and fix a complex coordinate $z = x + iy$ on that region. Assume:*

- *ψ has an* isolated simple zero *at z_0 and is nonzero on an annulus $A = \{r_1 < |z - z_0| < r_2\}$,*
- *$w = \partial_z^2 \log \psi$ is well-defined on A, and*
- *on A one can factor $\psi = (z - z_0)g$ with $g \neq 0$ and $\partial_z^2 \log g$ small compared to $(z - z_0)^{-2}$ (in a quantified sense, e.g. $|(z - z_0)^2\, \partial_z^2 \log g| \leq \varepsilon \ll 1$).*

Then on the subset of A where the probability current $\mathbf{J} = \mathrm{Im}(\bar{\psi}\, \nabla\psi)$ is nonzero, the current direction field $\mathbf{J}/|\mathbf{J}|$ approximately aligns with the QD-horizontal direction field determined by

$$\theta_{\mathrm{qd}} = -\tfrac{1}{2} \arg(w) \ (\mathrm{mod}\ \pi),$$

with an angle error that is expected to scale with ε.
Comment. *theorem 4.6 proves asymptotic alignment as $|z - z_0| \to 0$ under the local factorisation $\psi = (z - z_0)g$ with $g \neq 0$. The conjecture concerns extending this local mechanism to a finite annulus by requiring that the double-pole term in w dominate the remainder throughout A.*

Remark 4.8 In the strictly stationary 1D bound-state setting with a real eigenfunction, both the Bohmian velocity and the probability current vanish away from nodes. In that regime the conjecture is not about literal real-axis trajectory coincidence; it targets regimes with nonzero current (e.g. 2D vortices, scattering states, or time-dependent superpositions) where probability-current streamlines provide a nontrivial flow to compare against.

Remark 4.9 (Limitations and non-examples) The direction-field alignment suggested by the vortex class is not automatic for general nodal patterns. In particular, multi-node states can exhibit substantial misalignment between **J** and the QD-horizontal direction field even away from the nodes. The script `scripts/qd_vs_current_two_nodes.py` provides a concrete two-node test case where the misalignment histogram is broad rather than sharply peaked near zero; this should be read as evidence that any global foliation/trajectory statement requires additional hypotheses beyond analyticity and nonzero current. A comprehensive survey of singular and topological features of nodal wave patterns can be found in [10].

5 Nodal Singularities and Confinement

Near a node of multiplicity m, $w \sim -m/(z-\rho)^2$ (a double pole in w). Quadratic differential theory implies a distinguished local trajectory structure whose qualitative type depends on the leading coefficient and the chosen branch for $\sqrt{w}$.

Conjecture 5.1 (Nodal confinement from one-sided seam monotonicity (open problem)) *Assume the amplitude seam s satisfies a suitable one-sided transverse monotonicity condition on a node-free region (e.g. $\partial_\sigma s \geq c > 0$ on an open set U that does not contain zeros of ψ). Then nodal accumulation* inside *U should be obstructed under additional mild hypotheses.*
Motivation (heuristic). *Near a zero ρ of multiplicity m, one has $s = \log R \sim m \log|z-\rho| +$ smooth, so transverse derivatives necessarily change sign across a node; thus any monotonicity condition can only hold on a node-free region. However, the logarithmic singularity is locally integrable, so turning this into a contradiction for a pointwise bound on U is subtle. A natural route is potential theory: wherever $R > 0$, the seam identity eq. (2.6) yields $\Delta s + |\nabla s|^2 = -Q$. In regimes where $Q \geq 0$, this makes s subharmonic, and the maximum principle then constrains how large s can be on subdomains. Formulating and proving a clean "no interior accumulation" theorem along these lines is left as a concrete open problem.*

6 Stationary-State Degeneracy

When S is constant (real wave functions), $\nabla\tilde{s} \propto \nabla s$ and g may vanish where $\nabla s = 0$. The flow is stationary (velocity zero). The foliation picture remains well-defined: horizontal leaves collapse to level sets of s. The geometry is recovered in the limit of infinitesimal phase perturbations, where geodesics become short segments along level sets.

7 Supporting Numerical Computation

We use two complementary numerical illustrations. Both are implemented as reproducible Python scripts in the repository and generate the PDF figures included below (when present).

To quantify direction-field agreement we use the angle difference (mod π)

$$\Delta\theta := \theta_J - \theta_{\mathrm{qd}} \ (\mathrm{mod}\ \pi),$$

and report the alignment statistic

$$\alpha := \langle |\sin(\Delta\theta)| \rangle, \tag{7.1}$$

averaged over a grid after masking near nodes and regions with numerically negligible current. Table 1 summarises the outcomes for three representative states. The roughly three-order-of-magnitude separation between the vortex cases ($\alpha \sim 10^{-4}$) and the two-node case ($\alpha \approx 0.12$) shows that the single-vortex condition does real work: it is not merely smoothing a near-alignment that happens generically.

State	α from eq. (7.1)	RMS($\lvert\Delta\theta\rvert$) [deg]	95% quantile [deg]
Vortex $\psi = ze^{-\lvert z\rvert^2/2}$	1.01×10^{-4}	7.76×10^{-3}	1.45×10^{-2}
Shifted vortex $\psi = (z - z_0)e^{-\lvert z\rvert^2/2}$	1.11×10^{-4}	8.92×10^{-3}	1.81×10^{-2}
Two nodes $\psi = (z^2 - a^2)e^{-\lvert z\rvert^2/2}$	1.17×10^{-1}	1.40×10^{1}	2.91×10^{1}

Table 1 Direction-field alignment statistics for the three numerical tests in § 7 (grid-based comparison away from nodes; $\Delta\theta$ taken modulo π). The first two are near-perfectly aligned; the two-node case is a non-example that motivates additional hypotheses beyond analyticity and nonzero current

7.1 Harmonic-oscillator node geometry (structure only)

For the harmonic-oscillator first excited state $\psi_1(x) = \sqrt{2}\pi^{-1/4} x \exp(-x^2/2)$ (node at $x = 0$):

In the simplest analytic continuation $\psi_1(z) \propto z \exp(-z^2/2)$ one finds explicitly

$$w(z) = \partial_z^2 \log \psi_1(z) = -1 - \frac{1}{z^2},$$

so the node becomes a double pole of w at $z = 0$.

Figure 1 plots approximate horizontal trajectories of $w\,dz^2$ in the complex plane with a $\log|w|$ background, and marks the real axis as the configuration line. Since for a real stationary eigenstate the Bohmian velocity is identically zero away from nodes, this figure is included as a clean visualisation of how the double-pole structure of w organises the local foliation near a node, rather than as a trajectory-comparison test.

An implementation that generates fig. 1 is provided in `scripts/harmonic_qd_foliation.py`.

7.2 Vortex test (nonzero current; quantitative evidence)

In 2D one can choose states with a genuine circulating probability current. For the vortex-like state

$$\psi(x, y) = (x + iy) \exp(-(x^2 + y^2)/2),$$

we numerically compare probability-current streamlines to the quadratic-differential horizontal direction field derived from $w = \partial_z^2 \log \psi$. In this specific case the alignment can in fact be shown analytically (*exactly* away from the node); see theorem 4.5.

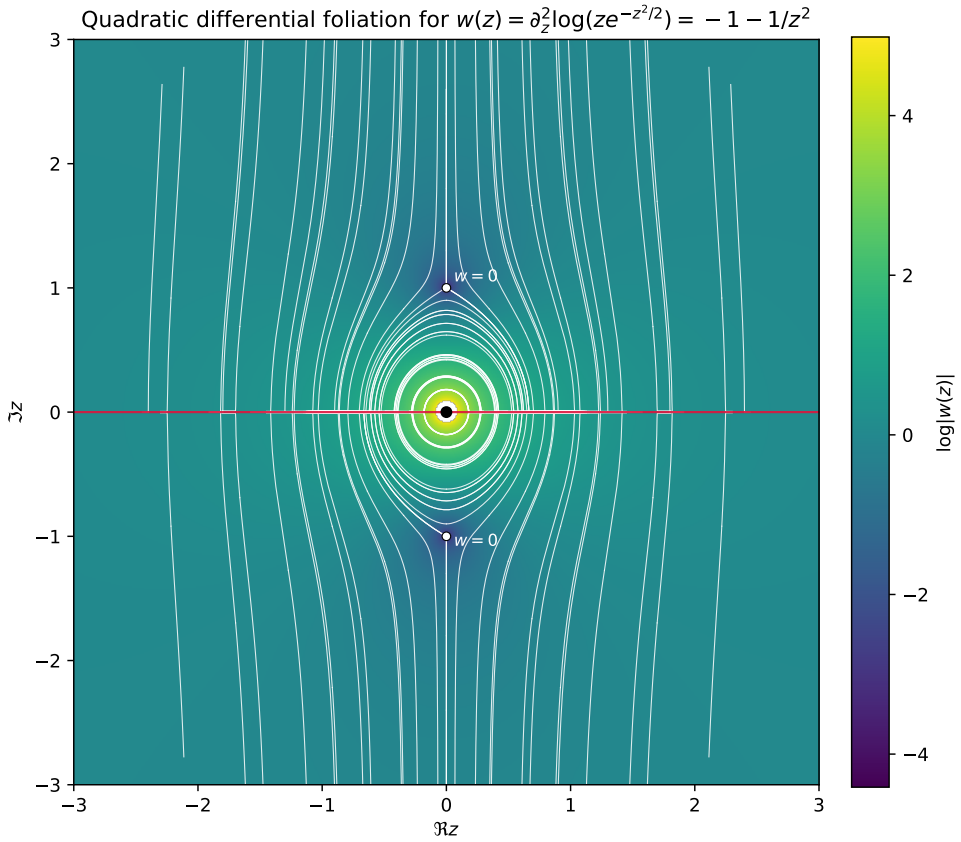


Fig. 1 Horizontal foliation of $w\,dz^2$ for the analytically continued harmonic-oscillator first excited state, plotted in the complex plane with a $\log|w|$ background

The angle-misalignment histogram in fig. 2 therefore serves as a numerical consistency check of the discretisation and streamline tracing, and as a benchmark for less symmetric examples where no closed-form alignment proof is available.

An implementation that generates fig. 2 is provided in `scripts/qd_vs_current_vortex.py`.

7.3 Shifted vortex test (symmetry-broken test)

To break the obvious rotational symmetry about the origin while keeping a single vortex node, we test

$$\psi(x, y) = (z - z_0)\exp(-|z|^2/2), \qquad z = x + iy,$$

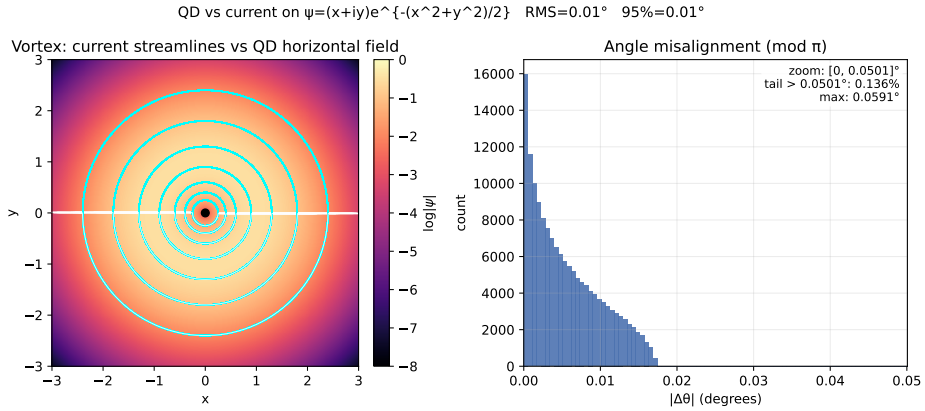


Fig. 2 2D vortex test: probability-current streamlines versus the quadratic-differential horizontal direction field derived from $w = \partial_z^2 \log \psi$, plus a histogram of the angle misalignment (mod π)

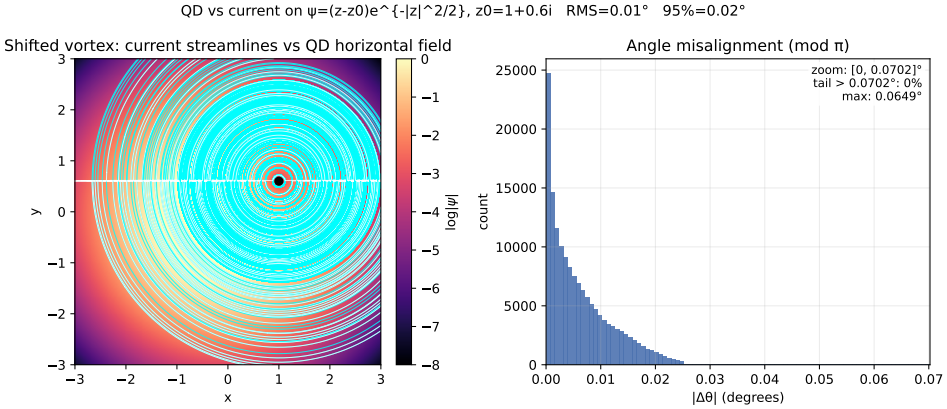


Fig. 3 Shifted vortex test: probability-current streamlines versus the quadratic-differential horizontal direction field derived from $w = \partial_z^2 \log \psi$, plus a histogram of the angle misalignment (mod π)

with a fixed off-centre node location $z_0 \neq 0$. This state has a nonzero circulating current around z_0 but a Gaussian envelope centered at the origin. The resulting misalignment histogram in fig. 3 is again sharply concentrated near zero, providing a simple robustness test that the observed alignment is not an artefact of placing the vortex at the origin. An implementation that generates fig. 3 is provided in `scripts/qd_vs_current_shifted_vortex.py`.

8 Discussion

This paper isolates three layers: (i) standard Bohm–Madelung identities expressed in seam variables ($s = \log R$), (ii) a seam-induced conformal factor $|\nabla \tilde{s}|^2$ (whose 1D

geodesic interpretation is necessarily reparametrisation-trivial), and (iii) a quadratic-differential organiser for nodal neighbourhoods that requires analytic continuation and careful branch conventions.

In this paper, (i) is fully explicit, while (ii)–(iii) are geometric proposals supported by local pole structure and by the numerical tests in section 7.

The current evidence supports a narrow message: in the single-vortex class the QD-horizontal direction field matches the probability-current direction field exactly (and remains numerically stable under translation of the vortex), and more generally theorem 4.6 shows that this mechanism holds asymptotically near any isolated simple node under a mild local factorisation hypothesis. However, multi-node states need not align away from nodes. Any correct global theorem therefore appears to require a "single-vortex dominance" hypothesis (or an equivalent condition ensuring that the local double-pole contribution to $w = \partial_z^2 \log \psi$ controls the direction field on a finite annulus).

Further directions include clarifying the precise statement relating foliation curves to configuration-space trajectories (including branch conventions), broadening the set of numerical tests beyond the single-vortex class, and exploring higher-dimensional analogues via level-set foliations of s.

Outlook. Concrete directions suggested by this dictionary include:

- 2D/3D level-set foliation theory for nodal lines/surfaces expressed in seam variables.
- Making one-sided "transverse monotonicity" criteria on s precise enough to yield geometric nodal theorems.
- Extending the quadratic-differential comparison to time-dependent wave packets (streamlines of the full current) and to scattering states (nonzero stationary current); Bohmian trajectory methods for time-dependent problems are reviewed in [6].
- Exploring links to geometric quantum mechanics and information geometry, where scalar potentials generate natural metrics on state spaces.

9 Conclusion

The seam variables provide a compact repackaging of the Bohm–Madelung decomposition, with the quantum potential arising directly from the curvature of $s = \log R$. A promising but still-developing picture connects nodal structure to the local trajectory geometry of a quadratic differential derived from $\log \psi$. Turning that picture into a theorem will require (at minimum) a precise map from the complex-plane foliation to configuration-space dynamics and a clean treatment of branch choices at nodes.

Statements and Declarations

Competing Interests. The author has no relevant financial or non-financial interests to disclose.

Funding. The author did not receive support from any organization for the submitted work.

Declaration of generative AI and AI-assisted technologies. During the preparation of this work the author used Grok 4.2, GPT-5.2, Gemini 3.1 Pro, and Claude Sonnet 4.6 in order to draft early versions of the manuscript, brainstorm and outline the revised manuscript, polish the exposition, and respond to reviewer feedback. After using these tools/services, the author reviewed and edited the content as needed and takes full responsibility for the content of the published article.

Code Availability

All figures and numerical alignment statistics reported in this manuscript are generated by reproducible Python scripts included in the companion repository at https://github.com/Roenbaeck/bohmian. For this version of the manuscript, the scripts correspond to repository state commit `9da134e`. See `README.md` in the repository for the exact commands used to generate each figure.

References

[1] D. Bohm, Phys. Rev. **85**, 166 (1952).

[2] E. Madelung, Z. Phys. **40**, 322 (1926).

[3] T. Takabayasi, Prog. Theor. Phys. **8**, 143 (1952).

[4] P. R. Holland, *The Quantum Theory of Motion* (Cambridge University Press, 1993).

[5] D. Dürr and S. Teufel, *Bohmian Mechanics* (Springer, 2013).

[6] R. E. Wyatt, *Quantum Dynamics with Trajectories: Introduction to Quantum Hydrodynamics* (Springer, 2005).

[7] K. Strebel, *Quadratic Differentials* (Springer, 1984).

[8] J. F. Nye and M. V. Berry, Proc. R. Soc. Lond. A **336**, 165 (1974).

[9] M. V. Berry and M. R. Dennis, Proc. R. Soc. Lond. A **456**, 2059 (2000).

[10] M. R. Dennis, K. O'Holleran, and M. J. Padgett, Prog. Opt. **53**, 293 (2009).

[11] V. Ovsienko and S. Tabachnikov, *Projective Differential Geometry Old and New: From Schwarzian Derivative to Cohomology of Diffeomorphism Groups* (Cambridge University Press, 2005).

[12] P. Di Francesco, P. Mathieu, and D. Sénéchal, *Conformal Field Theory* (Springer, 1997).